Journal of
Composites Science

MDPI

Article

Advancing Thermochromic Glass Durability: Reinforcing Thermosensitive Hydrogels with Enhanced Adhesion Techniques

Dewei Qian [1,2,3], Suili Peng [1,2,3], Tao Zhang [4], Liang Qin [4] and Weijia Wen [2,3,5,*]

[1] Division of Emerging Interdisciplinary Areas, Academy of Interdisciplinary Studies, The Hong Kong University of Science and Technology, Clear Water Bay, Kowloon, Hong Kong; dqianaa@connect.ust.hk (D.Q.); suili@connect.ust.hk (S.P.)
[2] Thrust of Advanced Materials, The Hong Kong University of Science and Technology (Guangzhou), Nansha, Guangzhou 511400, China
[3] Shenzhen-Hong Kong Collaborative Innovation Research Institute, The Hong Kong University of Science and Technology, Futian, Shenzhen 518000, China
[4] Chongqing Hewei Technology Co., Ltd., Chongqing 401120, China; tao.zhang@cqhwkj.com (T.Z.); 17830828599@163.com (L.Q.)
[5] Department of Physics, The Hong Kong University of Science and Technology, Clear Water Bay, Kowloon, Hong Kong
* Correspondence: phwen@ust.hk

Abstract: The growing use of glass in architecture has driven research into reducing its energy consumption. Thermochromic (TC) glass technology shows promise for enhancing building energy efficiency by regulating solar heat dynamically. Although TC glass helps reduce heat radiation, additional solutions like Low-E or vacuum glass are needed to control heat convection and conduction. Low-E glass, while effective in lowering heat transfer, may increase surface temperature. Thermosensitive hydrogels, known for their light-scattering properties at high temperatures, have been explored to complement TC glass. However, their stability at elevated temperatures remains a challenge, especially for applications requiring durability under varying weather conditions. This study proposes enhancing the adhesion between hydrogel and glass by introducing silica–oxygen bonds. As a result, TC glass demonstrates stable performance over 100 cycles within temperature ranges from 85 °C to 30 °C in summer and 40 °C to −20 °C in winter. Furthermore, by incorporating ethylene glycol, the freezing point of TC glass is reduced to −26 °C, rendering it suitable for use in colder regions. The implementation of TC glass effectively addresses the dual requirements of summer shading and winter heating in areas with both cold winters and hot summers, significantly reducing building energy consumption. This study contributes substantially to developing advanced intelligent building materials, paving the way for more sustainable architectural designs.

Keywords: thermochromic glass; hydrogel; silica–oxygen bonds; LCST

Citation: Qian, D.; Peng, S.; Zhang, T.; Qin, L.; Wen, W. Advancing Thermochromic Glass Durability: Reinforcing Thermosensitive Hydrogels with Enhanced Adhesion Techniques. *J. Compos. Sci.* **2024**, *8*, 371. https://doi.org/10.3390/jcs8090371

Academic Editor: Francesco Tornabene

Received: 6 August 2024
Revised: 11 September 2024
Accepted: 19 September 2024
Published: 20 September 2024

1. Introduction

Building energy efficiency has become a critical focus in the construction industry due to rising energy costs and increasing environmental concerns [1,2]. Among the various technologies aimed at improving building energy performance, thermochromic smart glass has garnered significant attention for its ability to dynamically modulate solar heat gain and enhance occupant comfort [3]. Vanadium dioxide [4,5], temperature-sensitive hydrogels [6–8], and liquid crystals [9,10] have been widely studied for their applications in thermochromic glass. By adjusting its transparency in response to external temperature changes, thermochromic smart glass effectively reduces the need for mechanical heating, ventilation, and air conditioning systems, leading to substantial energy savings and reduced greenhouse gas emissions [11–13]. Many researchers have focused on thermosensitive hydrogels due to their strong ability to regulate solar thermal radiation, making them a key

component in the study of building dynamics [14–16]. Despite its promising potential, a critical technical challenge has impeded the widespread adoption of thermochromic smart glass in building applications: inadequate adhesion between the thermochromic hydrogel and the glass substrate. The surface temperature of TC glass is influenced by several factors, including solar radiation intensity, ambient temperature, the characteristics of the glass itself (such as reflectivity, transmittance, and absorptivity), and the geographical location of the glass [17,18]. Under clear weather conditions, if the sun directly shines on the surface of the TC glass, its surface temperature can be from 20 to 40 °C higher than the ambient temperature [19–24]. At elevated temperatures, the weak adhesion between the hydrogel and glass often results in delamination or the formation of air bubbles within the hydrogel layer, which compromises both its optical properties and durability. Therefore, improving the adhesion between the thermochromic hydrogel and the glass substrate is crucial for enhancing the reliability and performance of thermochromic smart glass technology in building applications.

Researchers have explored treating the glass surface with silicon–oxygen compounds that react with acrylamide to enhance the adhesion between the hydrogel and the glass. Tian's team utilized silane coupling agents to modify the glass surface, adding extended chain siloxy functional groups that can be cross-linked with the hydrogel through topological entanglement [25]. This method forms long chains of covalent bonds on the glass, effectively increasing the adhesion between the hydrogel and the glass. As a result, a stable thermo-dimming glass is produced, maintaining stability after 100 color-changing cycles and transmittance. Professor Lu and his team proposed a general strategy for the solid adhesion of hydrogels, addressing the adhesion problem between hydrogels and various materials [26]. This strategy combines chemical adhesion and topological entanglement, allowing any hydrogel to be effectively bonded to the substrate. The key to this universal bonding strategy lies in polymer chains with multifunctional groups and triggerable cross-linking properties. These polymer chains can diffuse into the hydrogel network and cross-link upon triggering to form new topological entanglements. This newly formed network can bond hydrogels with other materials at the molecular scale, similar to stitches, without the need for a specific chemical design of the hydrogels. Liu and his team incorporated silane into hydrogels and elastomers [27]. In the presence of water, the alkoxy group in silane hydrolyzes to silanol, and two silanols can condense to form a siloxane bond. Silane copolymerizes into the hydrogel and elastomer networks for rapid hydrolysis, while the condensation between silanols occurs relatively slowly, providing sufficient time for processing before bonding. After processing, the silanol between the gel and elastomer networks condenses, covalently connecting the two materials to provide a strong bond. Many researchers focus on enhancing the substrate interface and hydrogel adhesion. Typically, the adhesion between hydrogel and glass is improved through substrate treatment followed by extension [28]. However, treating large pieces of glass for TC applications can be both time-consuming and resource-intensive, posing significant challenges for large-scale implementation. The extensive time required for proper treatment, along with the high consumption of resources, diminishes the feasibility of deploying TC glass on a broad scale. These challenges hinder the widespread adoption of TC glass in larger architectural projects and commercial applications, where efficiency and cost-effectiveness are crucial. Overcoming these barriers is essential for making TC glass a practical and sustainable solution for improving energy efficiency and occupant comfort in buildings. Addressing these issues will enable the more extensive use of TC glass, ultimately contributing to more sustainable building practices.

In this study, we enhanced the bonding strength between the glass substrate and hydrogel by incorporating silicon–oxygen bonds into the hydrogel matrix. By introducing a silane coupling agent that reacts with both polyacrylamide in the hydrogel and the glass surface, we significantly improved adhesion. This method effectively addresses adhesion challenges and enhances the overall performance of the hydrogel. By overcoming these critical adhesion limitations, we aim to promote the broader adoption of thermochromic

smart glass as a cost-effective and environmentally friendly solution for improving building energy efficiency and occupant comfort.

2. Materials and Methods

2.1. Materials

Acrylamide (AM): Acrylamide is a key monomer used in the polymerization process to form the polyacrylamide network.

Ethylene Glycol: This compound acts as a crosslinker and a plasticizer.

N, N′-Methylenebisacrylamide (BIS): BIS is a crosslinking agent that forms covalent bonds between acrylamide molecules.

Ammonium Persulfate (APS): APS is an initiator that decomposes under heat to produce free radicals.

N, N, N′, N′-Tetramethyl Ethylenediamine (TEMED): TEMED is a catalyst that accelerates the polymerization process initiated by APS, ensuring a more controlled and efficient formation of the hydrogel network.

γ-Isobutylene Propyl Trimethoxy Silane (γ-PTS): γ-PTS is a silane coupling agent used to improve the adhesion between the hydrogel matrix and other substrates, enhancing the stability and performance of the material, as shown in Figure 1.

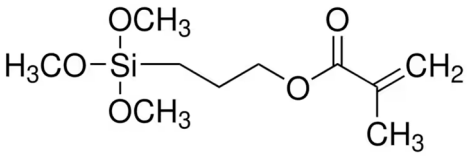

Figure 1. Chemical structure diagram of γ-PTS.

Triblock polyether (Molecular weight: 2000. As described in a previous paper [29,30]).

All the materials were purchased from Sigma-Aldrich (Shanghai, China) without further purification.

Ultrapure water (18.25 MΩ) was used throughout the experiments.

2.2. Thermochromic Hydrogel Synthesis

The synthesis of the thermochromic hydrogel involved the following steps: Triblock polyether, AM, BIS, APS, γ-PTS, and Ethylene glycol were dissolved in ultrapure water. The proportions of these materials were carefully determined based on the desired temperature-responsive properties.

Specifically, triblock polyether constituted 0.5–1% of the total mass of the aqueous solution, while AM accounted for 12% of the mass. BIS was included at 0.2% of the mass of AM, APS at 2% of the mass of the aqueous solution, and ethylene glycol ranged from 0 to 30% by mass relative to the ultrapure water. TEMED was added at 2.5% by mass relative to AM.

After completely dissolving all components, the solution temperature was lowered to below 10 °C. TEMED was then added to the solution under continuous agitation. Subsequently, the mixture was maintained under a pressure of −0.085 MPa for 20 min. This process resulted in the formation of a prepared hydrogel mixture. The hydrogel mixture was then transferred into a suitable container and cured at 60 °C for 1 h, solidifying it into the desired shape. The resulting thermochromic hydrogel exhibited the intended structural and functional properties for subsequent applications.

Due to its high water content, hydrogel tends to freeze at lower temperatures, adversely affecting the transparency of the glass. When frozen, the hydrogel expands, trapping air and forming bubbles, compromising TC glass's aesthetic and photothermal properties. Ethylene glycol, known for its efficacy in significantly lowering the freezing point of water, was employed in this study to adjust the hydrogel's freezing point.

2.3. Characterization

2.3.1. Photothermal Performance Test

The device was a lambda1050+ (Perkinelmer, Inc., Waltham, MA, USA) with a 150 mm integrating sphere. Sample preparation: The liquid was introduced into a double-layered glass with a 2 mm glass cavity (measuring 100 mm × 100 mm × 6 mm) and then subjected to a curing process at 60 °C for 1 h.

2.3.2. Hydrogel Mechanical Properties Test

We used an electric tensile testing machine. Dongguan Zhichou Precision Instrument Co., Ltd. (Dongguan, China) is the equipment manufacturer. Sample preparation: The mixed liquid was put in a cylindrical mold with a diameter and height of 60 mm. Then, the model was placed in a 60 °C oven for 1 h curing. After curing and cooling, the hydrogel could be obtained quickly and used to test its mechanical properties. The sample and test status are shown in Figures 2 and 3.

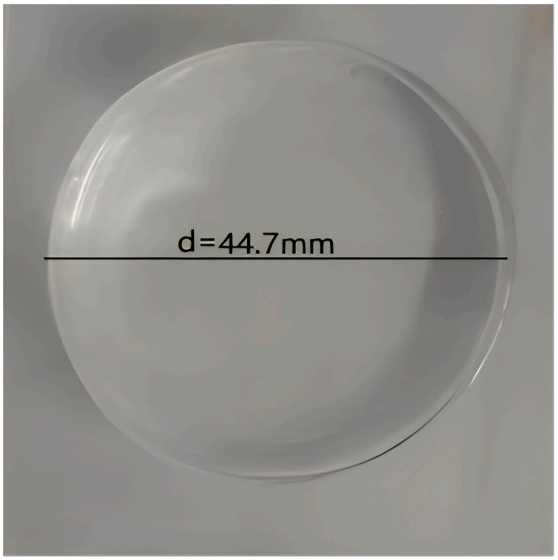

Figure 2. The shape of pressure resistance test hydrogel. Gel diameter: 44.7 mm.

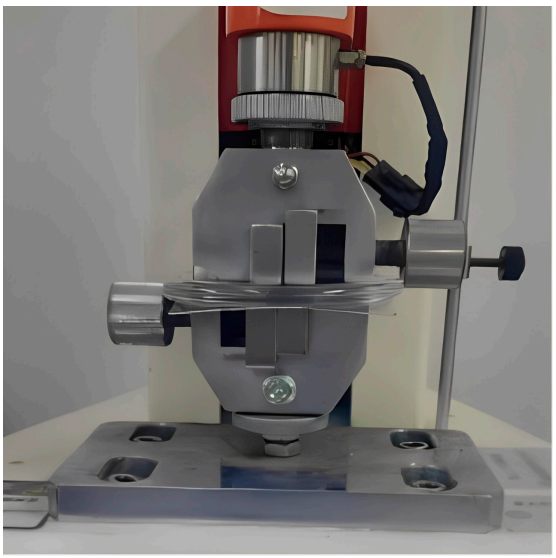

Figure 3. Pressure resistance test equipment. Test direction: downward. The test settings are as follows: Test speed: 10 mm/min. Preload speed: 100.0 mm/min. Compressed distance: 3 mm, 6 mm, 8 mm, and 10 mm.

2.3.3. Hydrogel Material Analysis and Sample Preparation

The hydrogel was initially cured in a 100 × 100 mm PET sample box with a hydrogel thickness of 2 mm at 60 °C for 1 h. After curing, the sample was placed in a vacuum freeze-drying machine (Zhengzhou Huachen Instrument Co., Ltd., Zhengzhou, China) to remove the water content. The freeze-drying process began by maintaining the sample at −30 °C for 2 h, followed by −10 °C for 4 h, with the vacuum pressure kept at ≤5 Pa. The temperature was then raised to 10 °C and held for 4 h, still under a vacuum pressure of ≤5 Pa. Finally, the temperature was increased to 40 °C and maintained for 10 h under the same vacuum conditions. After the freeze-drying process, the hydrogel samples were analyzed using Fourier Transform Infrared (FTIR) spectroscopy to study the chemical reactions within the freeze-dried hydrogel materials.

2.3.4. The Weather Resistance Test Consists of High- and Low-Temperature Cycles

The equipment manufacturer is Guangdong Hongzhan Technology Co., Ltd. (Maoming, China). The size of the sample was 300 × 300 mm. The TC glass's lower critical solution temperature (LSCT) was 25 °C.

3. Results and Discussion

3.1. Fourier Infrared Test

Fourier Transform Infrared (FTIR) spectroscopy was used to analyze the polysiloxane-modified siloxane-modified hydrogel, as shown in Figure 4.

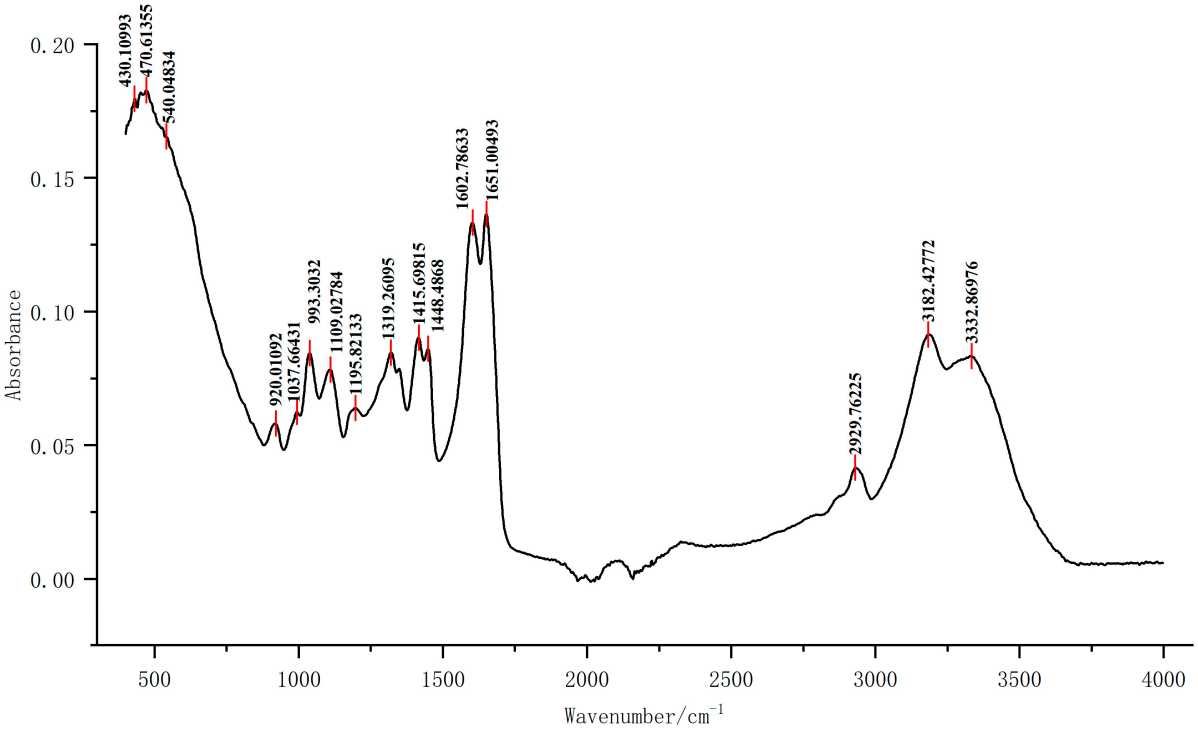

Figure 4. Fourier infrared image of a siloxane-modified hydrogel.

As shown in Table 1, significant absorption peaks were seen at 1602 cm^{-1} and 1651 cm^{-1}, corresponding to N-H bending and C=O stretching vibrations, respectively. These peaks confirm the presence of amide bonds, which are characteristic of the polyacrylamide hydrogel structure. Additionally, absorption peaks at 1415 cm^{-1} and 1448 cm^{-1}, attributed to C-N stretching vibrations of the primary amide bond, further corroborate the successful formation of the polyacrylamide hydrogel [31,32]. Furthermore, the FTIR analysis detected Si-O-C absorption peaks at 1109 cm^{-1} and 1195 cm^{-1}, indicating the incorporation of silicon–oxygen functional groups into the hydrogel matrix [33,34]. The

presence of these peaks signifies the successful integration of polysiloxane groups into the polyacrylamide network, enhancing the chemical bonding between the hydrogel and the glass substrate. The observed spectral features highlight the successful modification of the polyacrylamide hydrogel with polysiloxane groups, which is expected to improve the adhesion properties of the hydrogel. The incorporation of silicon–oxygen bonds facilitates robust interactions between the hydrogel and the glass surface, potentially addressing previous challenges related to adhesion and stability.

Table 1. FTIR spectrum analysis and interpretation.

Wavelength/cm^{-1}	Bond	Interpretation
2929	C-H	C-H bonds in the polyacrylamide.
1415~1448	C-N	C-N stretching vibration absorption peak.
1602	N-H	The N-H bending vibration absorption peak in polyacrylamide.
1651	C=O	The carbonyl stretching vibration peak of the amide group (–$CONH_2$) in polyacrylamide.
1109~1195	Si-O-C	Si-O-C bonds between the silane coupling agent and the polyacrylamide hydrogel.

3.2. Material Adhesion Test

In Figure 5a, the hydrogel without γ-PTS adheres to only one side of the glass, leaving no residual hydrogel on the opposite side when the cured glass is severed. In contrast, after the inclusion of γ-PTS, the hydrogel tears from the center when the laminated glass is separated, with both pieces of glass remaining adhered to the hydrogel. This improvement is attributed to the formation of silica–oxygen bonds in γ-PTS. The long-chain double bond in γ-PTS participates in the hydrogel polymerization reaction, forming a new silica–oxygen chemical bond between the γ-PTS and the silica in the glass, resulting in a stronger bond between the hydrogel and the glass, as shown in Figure 5c. The reaction between γ-PTS and water is as follows:

$$\gamma\text{-PTS (Si (OCH}_3))_3 + H_2O \rightarrow \gamma\text{-PTS-Si-OH} + 3CH_3OH$$

(**a**) (**b**) (**c**)

Figure 5. (**a**) TC glass without the addition of γ-PTS was separated. (**b**) TC glass with the addition of γ-PTS was separated. (**c**) Structure diagram of the reaction between γ-PTS and glass and its interaction with polyacrylamide.

Subsequently, the silanol groups on the glass and γ-PTS form siloxane bonds:

$$\text{Si-OH(Glass)} + \text{Si-OH}(\gamma\text{-PTS}) \rightarrow \text{Si-O-Si} + H_2O$$

This finding has significant implications for applications requiring strong bonding between materials. Understanding how specific chemical interactions enhance adhesion properties allows for the development of improved strategies to design advanced materials with superior performance characteristics. Further studies are needed to explore this phenomenon in greater detail and determine the optimal conditions for achieving maximum adhesion strength between hydrogels and glass substrates.

Architectural glass is subjected to temperature fluctuations, wind pressure, and constant vibrations in practical applications. Enhancing the adhesion between the hydrogel and glass is critical for ensuring that the hydrogel vibrates synchronously with the glass, thereby preventing separation due to vibrational forces. Moreover, incorporating silicon–oxygen bonds into the hydrogel network can modify its structure, resulting in a more compact and resilient network. As a result, when the glass experiences continuous vibrations induced by wind pressure, the hydrogel maintains excellent stability within the glass cavity. This improved stability is essential for preserving the integrity and performance of the glass–hydrogel composite under dynamic environmental conditions, extending its practical applicability in architectural settings.

3.3. Deformation Resistance of Materials

Architectural glass panels are particularly vulnerable to vibrations caused by fluctuating wind pressures, which can compromise both structural integrity and performance. To address this issue, a hydrogel with inherent compressibility was utilized. Extensive testing was conducted to assess the hydrogel's ability to recover its shape and maintain stability under compression, confirming its effectiveness in preserving structural integrity under stress. To further enhance the hydrogel's performance, a silica framework was incorporated into its matrix. The addition of silica not only improved the hydrogel's mechanical strength and durability but also increased its capacity for energy dissipation, thereby minimizing the transmission of vibrations to the glass panels. This synergistic interaction between the hydrogel and silica framework provides an effective solution for mitigating vibration-related challenges in architectural glass applications, ensuring long-term durability and reliability under dynamic environmental conditions.

As demonstrated in Table 2, hydrogels modified with γ-PTS exhibit significantly higher pressure generation under equivalent compression levels compared to their non-modified counterparts. This enhancement suggests that the γ-PTS modification improves the load-bearing capacity and compressive resistance of the hydrogels, indicating superior mechanical properties. The increased pressure response highlights the ability of γ-PTS-modified hydrogels to better withstand applied loads, which is critical for thermochromic glass applications in building construction, where maintaining structural integrity under varying pressure conditions is essential. When these hydrogels are integrated into glass structures, they play a vital role in mitigating displacement caused by wind pressure. The enhanced compressive strength of the γ-PTS-modified hydrogels helps to maintain the alignment and position of the glass, reducing the risk of structural failure or misalignment.

Table 2. Pressure resistance of hydrogels when compressed at different distances.

Sample	Gel Diameter/mm	Gel Height/mm	Compress 3 mm/N	Compress 6 mm/N	Compress 8 mm/N	Compress 10 mm/N
With γ-PTS	44.7 mm	15.4 mm	0.0612 0.0603 0.0611	0.2007 0.1993 0.2013	0.7667 0.7609 0.7653	1.577 1.560 1.580
Without γ-PTS	44.7 mm	15.5 mm	0.0465 0.0430 0.0453	0.1322 0.1331 0.1325	0.3600 0.3621 0.3611	0.9750 0.0980 0.0985

Additionally, as shown in Table 3, γ-PTS-containing hydrogels exhibit rapid recovery to their original shape after a 10 mm compression, demonstrating a high degree of elastic recovery. This property is essential for materials subjected to dynamic environments where frequent or variable compression may occur. The hydrogel's ability to quickly revert to its original form ensures that it maintains both functional integrity and performance, even after repeated or prolonged deformation. This rapid recovery extends the material's lifespan and ensures the thermochromic glass's sustained effectiveness, preserving its optical and structural properties over time. The elastic recovery characteristic is particularly advantageous for construction applications where long-term durability and reliability are paramount. Overall, incorporating γ-PTS into the hydrogel matrix significantly enhances its mechanical properties and deformation-recovery capabilities, making it a robust solution for improving the performance of thermochromic glass in architectural applications.

Table 3. The time required for hydrogel recovery when compressed to 10 mm.

Sample	Gel Diameter/mm	Gel Height/mm	Recovery Time/1 min	Recovery Time/5 min	Recovery Time/1 h
With γ-PTS	44.7	15.4	13.96 mm 14.62 mm 13.06 mm	14.39 mm 14.07 mm 14.16 mm	15.3 mm 15.32 mm 15.23 mm
Without γ-PTS	44.7	15.5	7.77 mm 6.8 mm 8.9 mm	12.35 mm 11.65 mm 12.23 mm	15.36 mm 14.99 mm 15.39 mm

3.4. Freezing Resistance of the Material

The freezing point of hydrogels can be significantly lowered by the addition of ethylene glycol due to the presence of its hydroxyl groups, which disrupt hydrogen bonding between water molecules and inhibit ice crystal formation. Ethylene glycol is known for its effectiveness in preventing ice crystal growth and aggregation, thus reducing the freezing point of hydrogels more efficiently compared to other cryoprotectants [35]. For instance, glycerol, which is also commonly used to lower the freezing point of hydrogels due to its low toxicity, is less effective than ethylene glycol at equivalent concentrations [36]. In regions with extremely cold winters and hot summers, temperatures can drop below −25 °C and, in some areas, even below −30 °C. Consequently, addressing the issue of hydrogel freezing at such low temperatures is crucial for ensuring the reliability and performance of hydrogels in these environments. As indicated in Table 4, the addition of 30% ethylene glycol can reduce the hydrogel's freezing point to −26 °C. This reduction effectively accommodates most applications in regions experiencing cold winters and hot summers. While ethylene glycol significantly lowers the freezing point of hydrogels, it also impacts the LCST of thermosensitive hydrogels. Ethylene glycol's interference with hydrogen bonding results in a decreased LCST, which can alter the temperature-responsive behavior of the hydrogel. For practical applications requiring thermochromic glass with a higher LCST, it is essential to adjust the hydrogel's formulation to balance the freezing point reduction with

the desired LCST. Therefore, while ethylene glycol is effective in addressing freezing point issues, careful consideration and adjustment of the hydrogel's LCST are necessary to ensure optimal performance in thermochromic applications. Balancing these factors is crucial for developing hydrogels that meet the specific requirements of various environmental conditions while maintaining functional efficacy.

Table 4. Effects of different contents of ethylene glycol on the freezing point of hydrogel.

Sample No	Ethylene Glycol/%	Freezing Point/°C
1	0	−10
2	5	−14
3	10	−16
4	20	−20
5	30	−26

3.5. TC Glass Parameters

As shown in Table 5, the efficacy of the shading mechanism in TC glass, characterized by its LCST, is optimized within a temperature range of 15 °C. When the LCST is set to a lower threshold, the TC glass allows the transmission of both ultraviolet (UV) and visible spectra of sunlight, resulting in a higher SHGC. Specifically, with a visible light transmittance of 0.882, the TC glass exhibits superior visibility and daylighting properties in its transparent phase compared to similar thermosensitive hydrogel-based intelligent glass systems [37]. This high transmittance enables more solar heat to enter the room, reducing the need for supplementary heating energy during winter. Conversely, when the LCST is set higher, the TC glass restricts the passage of visible and ultraviolet light. Under these conditions, the SHGC of the TC glass is significantly reduced, with a ΔSHGC of 0.436. This effectively blocks most of the solar radiation, thereby decreasing the energy consumption required for air conditioning and cooling during hotter periods. Additionally, Table 4 highlights that, as the temperature of the TC glass increases from 20 °C to 50 °C, the ultraviolet transmittance decreases from 0.8421 to 0.128. This substantial reduction in UV transmittance underscores the TC glass's ability to provide effective shading and control over UV radiation. By limiting UV light entering the room, the TC glass helps mitigate issues such as the fading and aging of indoor materials, thereby preserving the integrity of furnishings and reducing maintenance costs. The ability of TC glass to adjust its optical properties based on temperature makes it a highly effective solution for managing solar heat gain and UV exposure. The adaptability of TC glass enhances energy efficiency by optimizing heating and cooling demands and protecting interior environments from UV damage. This dual functionality makes TC glass a valuable component in sustainable building design, balancing comfort and energy efficiency across varying climatic conditions.

Table 5. Photothermal parameters of TC glass with LCST of 25 °C at different temperatures.

LCST	Test Temperature	Visible Transmittance (T_{vis})	Visible Light Reflectance (R_{vis})	Ultraviolet Transmittance (T_{uv})	Solar Heat Gain Coefficient (SHGC)	Solar Absorptivity
25 °C	20 °C	0.882	0.0848	0.8421	0.766	0.2377
	30 °C	0.1771	0.3281	0.1437	0.339	0.6163
	40 °C	0.1685	0.3452	0.1359	0.33	0.6103
	50 °C	0.1712	0.3470	0.1380	0.331	0.6069

As illustrated in Figure 6a, when the surface temperature of the TC glass is below its LCST, most infrared and ultraviolet rays within the solar spectrum, ranging from 400 nm to 1400 nm, pass through the glass into the interior space. However, once the temperature exceeds the LCST, the glass effectively blocks a significant portion of infrared rays, extending from 200 nm to 2500 nm, preventing their entry into the room. Furthermore,

when the surface temperature surpasses 40 °C, the transmittance of the solar spectrum tends to stabilize. Figure 5b demonstrates the reflectance of TC glass at various temperatures. Below the LCST, the reflectance is comparable to that of standard glass, with relatively low values. In contrast, above the LCST, reflectance increases significantly for sunlight in the range of from 400 nm to 1500 nm. Similar to transmittance, the reflectance stabilizes once the temperature exceeds 40 °C.

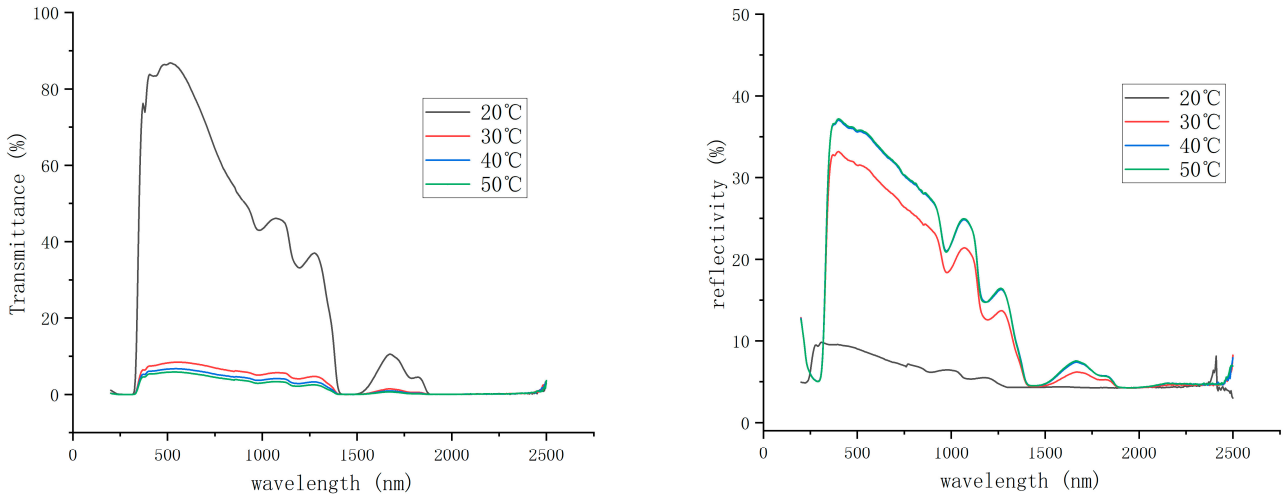

(**a**) (**b**)

Figure 6. Solar Transmittance and reflectivity of TC glass at various temperatures: (**a**) transmission spectrum. (**b**) Reflection spectrum.

When the temperature surpasses the LCST, the polymer chains within the hydrogel undergo a transition from a hydrophilic to a hydrophobic state, leading to microphase separation. This results in a heterogeneous refractive index distribution, which causes extensive scattering of visible light. Consequently, sunlight is diffused, reducing glare and direct solar penetration while maintaining a soft, natural lighting environment. Additionally, the structural changes in the hydrogel improve its ability to reflect and block infrared radiation, thereby reducing solar heat gain and enhancing energy efficiency in warmer climates. Collectively, Figure 6a,b indicates that TC glass achieves optimal performance around 25 °C, with an effective temperature range of approximately 15 °C. Notably, specific studies have observed that thermochromic materials transition from transparency to full coloration at around 5 °C [38]. However, for practical applications, further empirical evaluation is needed to assess the full implications of the color transition range, particularly regarding its impact on building energy conservation and overall utilization efficiency.

3.6. Stability of TC Glass

During the summer cycle, the temperature is 30 °C for 6 h, followed by 85 °C for 12 h. The cycle occurs 50 times [38,39]. During the winter cycle, the temperature is 40 °C for 6 h, followed by −20 °C for 12 h. The cycle occurs 50 times.

After undergoing a cycle of high and low temperatures, the 300 mm × 300 mm sample remained intact, as depicted in Figure 7. This indicates that the TC glass demonstrates substantial stability under extreme temperature conditions. In summer, particularly in regions with high solar irradiation, the surface temperature of TC glass can be significantly affected by solar thermal radiation. Tests indicate that the surface temperature of TC glass can exceed the ambient temperature by as much as 30 °C. During peak summer hours, from 11 am to 5 pm, the glass on the top surface is exposed to elevated temperatures. Therefore, verifying the high-temperature stability of TC glass during the summer months is crucial for its application in architectural contexts. Actual engineering tests have confirmed that

the product maintains high structural integrity at elevated temperatures, specifically up to 85 °C, which is essential for its application in high-temperature and high-radiation areas. This is evidenced by the high strength observed in the high-temperature environment, ensuring the product's suitability for architectural use under these conditions. Figure 7a illustrates that in the absence of γ-PTS, numerous irregular bubbles form on the glass surface after the high- and low-temperature cycles. These bubbles significantly compromise the aesthetic and functional quality of the product when used in construction. Prolonged exposure to solar radiation can lead to photo-oxidative aging, causing the TC glass to develop a yellow tint over time. Incorporating γ-PTS into the hydrogel formulation has been shown to mitigate these issues, enhancing the thermal and photostability of the TC glass. This additive plays a critical role in preventing bubble formation and discoloration, thereby maintaining the clarity and performance of the glass under extended exposure to harsh environmental conditions.

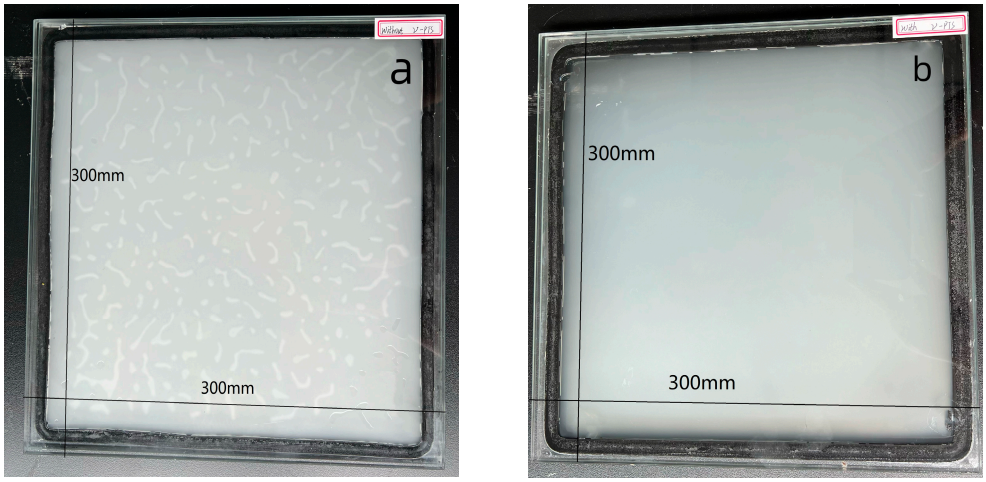

(**a**) (**b**)

Figure 7. Aging test of samples at high and low temperatures (Size: 300 mm × 300 mm): (**a**) TC glass without γ-PTS. (**b**) TC glass with γ-PTS.

4. Conclusions

In this paper, we have increased the adhesion between a hydrogel and glass by introducing γ-PTS into the hydrogel. This study proposed strengthening the adhesion between hydrogel and glass by introducing a silicon–oxygen bond and forming a stable silicon oxidation bond. The experimental results show that the modified TC glass still shows stable operating performance over 100 cycles. In addition, by adding ethylene glycol, the freezing point of TC glass is reduced to −26 °C, making its application in cold areas possible. The results show that TC glass technology can effectively achieve summer shading and winter heating in cold and hot summer areas, significantly reducing the energy consumption of buildings. Especially in cold winter and hot summer areas, the SHGC difference between winter and summer can reach more than 0.4, which can replace the active outdoor shading in the existing technology. This research not only provides a new idea for the development of intelligent building materials but also lays a solid foundation for the design and application of green buildings in the future.

Author Contributions: Conceptualization, D.Q. and W.W.; data curation, D.Q. and T.Z.; formal analysis, D.Q., S.P., T.Z. and L.Q.; funding acquisition, W.W.; methodology, D.Q.; project administration, W.W.; resources, W.W.; supervision, W.W.; validation, D.Q. and L.Q.; visualization, D.Q. and S.P.; writing—original draft, D.Q.; writing—review and editing, D.Q. and S.P. All authors have read and agreed to the published version of the manuscript.

Funding: This project is funded by Hetao Shenzhen-Hong Kong Science and Technology Innovation Cooperation Zone under grant HZQB-KCZYB-2020083 and the Hong Kong ITF grant MRP/084/20.

Data Availability Statement: The data are contained within the article.

Conflicts of Interest: The author Tao Zhang was employed by the company Chongqing Hewei Technology Co., Ltd. The remaining authors declare that the research was conducted in the absence of any commercial or financial relationships that could be construed as a potential conflicts of interest.

References

1. Anonymous. Max El Mann: Moving Towards Zero-Emission Building Construction. CE Noticias Financieras. 2023. Available online: http://ezproxy.ust.hk/login?url=https://www.proquest.com/wire-feeds/max-el-mann-moving-towards-zero-emission-building/docview/2829062701/se-2 (accessed on 22 June 2023).
2. Anonymous. U.N. Environment Programme's Global Alliance for Buildings and Construction Issues Report Entitled 'Towards a Zero-Emissions, Efficient and Relilient Buildings and Construction Sector'. Targeted News Service. 2021. Available online: http://ezproxy.ust.hk/login?url=https://www.proquest.com/wire-feeds/u-n-environment-programmes-global-alliance/docview/2601698183/se-2 (accessed on 31 December 2021).
3. Ke, Y.; Zhou, C.; Zhou, Y.; Wang, S.; Chan, S.H.; Long, Y. Emerging Thermal-Responsive Materials and Integrated Techniques Targeting the Energy-Efficient Smart Window Application. *Adv. Funct. Mater.* **2018**, *28*, 1800113. [CrossRef]
4. Chen, S.; Wang, Z.; Ren, H.; Chen, Y.; Yan, W.; Wang, C.; Li, B.; Jiang, J.; Zou, C. Gate-controlled VO_2 phase transition for high-performance smart windows. *Sci. Adv.* **2019**, *5*, eaav6815. [CrossRef] [PubMed]
5. Kuhl, F.; Becker, M.; Benz, S.L.; Hauptmann, J.; Kessler, J.; Chatterjee, S.; Polity, A.; Klar, P.J. Embedding Quaternary V_{1-x-y} Sr_x W_yO_2 into Multilayer Systems to Enhance Its Thermochromic Properties for Smart Glass Applications. *ACS Appl. Electron. Mater.* **2022**, *4*, 513–520. [CrossRef]
6. Xu, Z.; Wang, S.; Hu, X.; Jiang, J.; Sun, X.; Wang, L. Sunlight-Induced Photo-Thermochromic Supramolecular Nanocomposite Hydrogel Film for Energy-Saving Smart Window. *Sol. RRL* **2018**, *2*, 1800204. [CrossRef]
7. Wu, M.; Shi, Y.; Li, R.; Wang, P. Spectrally Selective Smart Window with High Near-Infrared Light Shielding and Controllable Visible Light Transmittance. *ACS Appl. Mater. Interfaces* **2018**, *10*, 39819–39827. [CrossRef]
8. Zhang, L.; Du, Y.; Xia, H.; Xia, F.; Yang, G.; Gao, Y. HPC-PAA hydrogel smart windows with and without $Cs_{0.32}WO_3$: High solar modulation ability and luminous transmittance. *Ceram. Int.* **2022**, *48*, 37122–37131. [CrossRef]
9. Pan, G.; Cao, H.; Guo, R.; Li, W.; Guo, J.; Yang, Z.; Huang, W.; He, W.; Liang, X.; Zhang, D.; et al. A polymer stabilized liquid crystal film with thermal switching characteristics between light transmission and adjustable light scattering. *Opt. Mater.* **2009**, *31*, 1163–1166. [CrossRef]
10. Zhang, W.; Lub, J.; Schenning, A.P.; Zhou, G.; de Haan, L.T. Polymer stabilized cholesteric liquid crystal siloxane for temperature-responsive photonic coatings. *Int. J. Mol. Sci.* **2020**, *21*, 1803. [CrossRef]
11. Xu, G.; Xia, H.; Chen, P.; She, W.; Zhang, H.; Ma, J.; Ruan, Q.; Zhang, W.; Sun, Z. Thermochromic Hydrogels with Dynamic Solar Modulation and Regulatable Critical Response Temperature for Energy-Saving Smart Windows. *Adv. Funct. Mater.* **2022**, *32*, 2109597. [CrossRef]
12. Liu, S.; Li, Y.; Wang, Y.; Du, Y.; Yu, K.M.; Yip, H.-L.; Jen, A.K.Y.; Huang, B.; Tso, C.Y. Mask-inspired moisture-transmitting and durable thermochromic perovskite smart windows. *Nat. Commun.* **2024**, *15*, 876. [CrossRef]
13. Shang, J.; Zhang, Y.; Zhang, J.; Zhang, X.; An, Q. Hydrogel-Based Stimuli-Responsive Radiative and/or Evaporative Cooling Materials for Carbon Neutrality. *ACS Energy Lett.* **2024**, *9*, 594–626. [CrossRef]
14. Chen, G.; Wang, K.; Yang, J.; Huang, J.; Chen, Z.; Zheng, J.; Wang, J.; Yang, H.; Li, S.; Miao, Y.; et al. Printable Thermochromic Hydrogel-Based Smart Window for All-Weather Building Temperature Regulation in Diverse Climates. *Adv. Mater.* **2023**, *35*, e2211716. [CrossRef] [PubMed]
15. Guo, R.; Shen, Y.; Chen, Y.; Cheng, C.; Ye, C.; Tang, S. KCA/Na_2SiO_3/PNIPAm hydrogel with highly robust and strong solar modulation capability for thermochromic smart window. *Chem. Eng. J.* **2024**, *486*, 150194. [CrossRef]
16. Mohammad, N.M.; Zhang, Y.; Xu, W.; Aranke, S.S.; Carne, D.; Deng, P.; Du, F.; Ruan, X.; Li, T. Highly Tunable Cellulosic Hydrogels with Dynamic Solar Modulation for Energy-Efficient Windows. *Small* **2024**, *20*, 2303706. [CrossRef]
17. Bhupathi, S.; Wang, S.; Wang, G.; Long, Y. Porous vanadium dioxide thin film-based Fabry−Perot cavity system for radiative cooling regulating thermochromic windows: Experimental and simulation studies. *Nanophotonics* **2024**, *13*, 711–723. [CrossRef]
18. Lee, S.; Song, S. Energy efficiency, visual comfort, and thermal comfort of suspended particle device smart windows in a residential building: A full-scale experimental study. *Energy Build.* **2023**, *298*, 113514. [CrossRef]
19. Palomar, T.; Silva, M.; Vilarigues, M.; Cardoso, I.P.; Giovannacci, D. Impact of solar radiation and environmental temperature on Art Nouveau glass windows. *Herit. Sci.* **2019**, *7*, 82. [CrossRef]
20. Kapur, N.K. A comparative analysis of the radiant effect of external sunshades on glass surface temperatures. *Sol. Energy* **2004**, *77*, 407–419. [CrossRef]
21. Akhtar, N.; Mullick, S.C. Effect of absorption of solar radiation in glass-cover (s) on heat transfer coefficients in upward heat flow in single and double glazed flat-plate collectors. *Int. J. Heat Mass Transf.* **2012**, *55*, 125–132. [CrossRef]
22. Hodder, S.G.; Parsons, K. The effects of solar radiation on thermal comfort. *Int. J. Biometeorol.* **2007**, *51*, 233–250. [CrossRef]
23. Gürtürk, M.; Benli, H.; Ertürk, N.K. Determination of the effects of temperature changes on solar glass used in photovoltaic modules. *Renew. Energy* **2020**, *145*, 711–724. [CrossRef]

24. Song, B.; Bai, L.; Yang, L. The Effects of Exterior Glazing on Human Thermal Comfort in Office Buildings. *Energies* **2024**, *17*, 776. [CrossRef]
25. Tian, J.; Peng, H.; Du, X.; Wang, H.; Cheng, X.; Du, Z. Durable, broadband-light-manageable thermochromic hydrogel with adjustable LCST for smart windows application. *Prog. Org. Coat.* **2021**, *157*, 106287. [CrossRef]
26. Gao, Y.; Chen, J.; Han, X.; Pan, Y.; Wang, P.; Wang, T.; Lu, T. A Universal Strategy for Tough Adhesion of Wet Soft Material. *Adv. Funct. Mater.* **2020**, *30*, 2003207. [CrossRef]
27. Liu, Q.; Nian, G.; Yang, C.; Qu, S.; Suo, Z. Bonding dissimilar polymer networks in various manufacturing processes. *Nat. Commun.* **2018**, *9*, 846. [CrossRef]
28. Liu, J.; Jiang, Z.; Li, Y.; Kang, G.; Qu, S. Stability of hydrogel adhesion enabled by siloxane bonds. *Eng. Fract. Mech.* **2022**, *271*, 108662. [CrossRef]
29. Qian, D.; Yang, S.; Wang, X.; Tian, Y.; Wen, W. Thermosensitive Scattering Hydrogels Based on Triblock Poly-Ethers: A Novel Approach to Solar Radiation Regulation. *Polymers* **2023**, *16*, 8. [CrossRef]
30. Madry, H.; Gao, L.; Rey-Rico, A.; Venkatesan, J.K.; Müller-Brandt, K.; Cai, X.; Goebel, L.; Schmitt, G.; Speicher-Mentges, S.; Zurakowski, D.; et al. Thermosensitive Hydrogel Based on PEO–PPO–PEO Poloxamers for a Controlled In Situ Release of Recombinant Adeno-Associated Viral Vectors for Effective Gene Therapy of Cartilage Defects. *Adv. Mater.* **2020**, *32*, e1906508. [CrossRef]
31. Chen, J.; Li, B.; Ma, X.; Zhou, S.; Gu, Q.; Bian, H.; Luo, Z. Modified lignin-induced composite hydrogels with good mechanical properties, adhesion, and UV resistance for strain sensors. *J. Appl. Polym. Sci.* **2023**, *140*, e54643. [CrossRef]
32. Jeong, Y.J.; Chathuranga, K.; Lee, J.S.; Park, W.H. Eco-friendly starch-based hydrogels with improved adhesion, antioxidant, and antimicrobial properties as wood adhesives. *Cellulose* **2023**, *30*, 7905–7921. [CrossRef]
33. Glad, B.E.; Kriven, W.M. Geopolymer with Hydrogel Characteristics via Silane Coupling Agent Additives. *J. Am. Ceram. Soc.* **2014**, *97*, 295–302. [CrossRef]
34. Franklin, D.S.; Guhanathan, S. Performance of silane-coupling agent-treated hydroxyapatite/diethylene glycol-based pH-sensitive biocomposite hydrogels. *Iran. Polym. J.* **2014**, *23*, 809–817. [CrossRef]
35. Azmi Roslan, A.M.; Tukiman, N.; Ibrahim, N.N.; Juanil, A.R. The effects of ethylene glycol to ultrapure water on its specific heat capacity and freezing point. *J. Appl. Environ. Biol. Sci.* **2017**, *7*, 54–60.
36. Fan, X.; Zhou, W.; Chen, Y.; Yan, L.; Fang, Y.; Liu, H. An Antifreezing/Antiheating Hydrogel Containing Catechol Derivative Urushiol for Strong Wet Adhesion to Various Substrates. *ACS Appl. Mater. Interfaces* **2020**, *12*, 32031–32040. [CrossRef]
37. Feng, Y.; Ma, W.; Li, H.; Yang, M.; Yu, Y.; Liu, S.; Zeng, X.; Huang, F.; Yang, Y.; Li, Z. Phase-Changing Polymer Film for Smart Windows with Highly Adaptive Solar Modulation. *ACS Appl. Mater. Interfaces* **2023**, *15*, 5836–5844. [CrossRef] [PubMed]
38. Chen, F.; Wu, X.; Lu, G.; Nie, J.; Zhu, X. Thermochromic Hydrogels with Adjustable Transition Behavior for Smart Windows. *ACS Appl. Mater. Interfaces* **2024**, *16*, 21013–21023. [CrossRef]
39. Tian, J.; Jin, C.; Wu, X.; Liao, C.; Xie, J.; Luo, Y. Synthesis of temperature- and humidity-induced dual stimulation film PU-PNIPAmn and its independent film formation as a smart window application. *RSC Adv.* **2023**, *13*, 8923–8933. [CrossRef]